Periodic forcing of a mathematical model of the eukaryotic cell cycle

Dorjsuren Battogtokh* and John J. Tyson
Department of Biology, Virginia Polytechnic Institute and State University, Blacksburg, Virginia 24061-0106, USA
(Received 18 September 2005; published 18 January 2006)

In a differential equation model of the molecular network governing cell growth and division, cell cycle phases and transitions through checkpoints are associated with certain bifurcations of the underlying vector field. If the cell cycle is driven by another rhythmic process, interactions between forcing and bifurcations lead to emergent orbits and oscillations. In this paper, by varying the amplitude and frequency of forcing of the synthesis rates of regulatory proteins and the mass growth rate in a minimal model of the eukaryotic cell cycle, we study changes of the probability distributions of interdivision time and mass at division. By computing numerically the Lyapunov exponent of the model, we show that the splitting of probability distributions is associated with mode-locked solutions. We also introduce a simple, integrate-and-fire model to analyze mode locking in the cell cycle.

DOI: 10.1103/PhysRevE.73.011910 PACS number(s): 87.17.−d, 05.45.−a, 82.40.Bj

I. INTRODUCTION

Rhythmic processes are ubiquitous in living organisms [1–4], for example, the beating heart, the daily cycles of waking and sleeping, and the physiological rhythms controlling the growth and proliferation of cells. Biological rhythms interact with each other as well as with the outside environment. At the cellular or molecular level, one rhythmic process can be forced by another. For instance, recent experiments reveal that the intracellular circadian clock can influence the cell-division cycle directly and unidirectionally in proliferating cells [5].

Significant research efforts have been devoted to uncovering the molecular mechanisms of the eukaryotic cell cycle [6] and circadian rhythms [7]. Detailed mathematical models for these rhythms have been developed [8–11]. In light of the recent report on cell cycle events driven by the circadian clock [14], and experiments on forcing the cell cycle by heat [15], light [16], and hypertonic stress [17], we have initiated a mathematical study of forced cell cycle oscillations. Mathematical modeling has proven useful in suggesting cell cycle experiments [12,13].

Controlling biochemical regulatory systems by periodic forcing in model systems has been a very active research field [21–30], demonstrating that forced oscillations display resonance and chaos, whose characteristics and signatures depend on biological specificities and nonlinearities in the mathematical models. As far as cell cycle modeling is concerned, there are two specific properties that interest us in regard to periodic forcing [31–33]. First, in these models, cell cycle phases G1/S/G2/M are not phases of a limit cycle oscillator. Progression through the cell cycle and cell divison are controlled by checkpoints which abruptly change the state of the control system from one phase to the next. Thus, responses to a periodic signal may be drastically different in different phases of the cell cycle. Secondly, as the cell cycle model can display birhythmicity, periodic forcing may switch oscillations between two stable orbits, leading to complexities that cannot occur in forced limit cycle oscillators.

The goal of this paper is to show that in a mathematical model of the cell cycle, the interdivision time and the mass at division can be controlled by the frequency and amplitude of periodic forcing. This paper is organized as follows. The next section gives a short introduction to a model that describes cell growth and division. In Sec. III, we study the cell cycle engine alone, considering the mass of the cell as a fixed parameter. Here, by using bifurcation diagrams, we analyze the possible shifts of bifurcation points due to forcing. In Sec. IV, we simulate a forced cell cycle model which takes into account the mass growth and cell division rules. We identify emergent oscillations due to period doubling and toruslike bifurcations, as well as the switching between bistable orbits. We show that, depending on the parameters of forcing, the probability distributions of interdivision time and mass at division can split into isolated distributions. In Sec. V, by computing the Lyapunov exponent of the minimal model, we show that splitting of the probability distribution is associated with the locking of the cell division cycle to the frequency of forcing. In this section, we also study mode locking in forced cell cycle oscillations by a simple, integrate, and fire model. By analyzing its Lyapunov exponents, we show that the mode-locking window is larger in the integrate and fire model. The last section is devoted to discussion.

II. A CELL CYCLE MODEL

A cell cycle model developed by Chen, Novak, Tyson, and co-workers [8,32,35] can be written in a compact form as

$$\frac{d\mathbf{x}}{dt} = Q(\mathbf{x},\mathbf{k},m), \tag{1}$$

$$\frac{dm}{dt} = \mu m, \tag{2}$$

where $\mathbf{x}$ is a vector of chemical concentrations controlling cell cycle events, m is the cell mass, $\mathbf{k}$ is a vector of the

*Corresponding author. Electronic address: dbattogt@vt.edu

TABLE I. Model parameters.

Rate constants (min^{-1})						
$k_1=0.002$	$k_2=0.053$	$k_3=0.01$	$k_4=2$	$k_5=0.05$	$k_6=0.04$	$k_7=1.5$
$k_8=0.19$	$k_9=0.64$	$k_{10}=0.005$	$k_{11}=0.07$	$k_{12}=0.08$	$\mu=0.005\,776$	
Other parameters (dimensionless)						
$P=0.15$	$J_1=0.05$	$J_2=0.01$	$\tau=0.5$			
Interdivision time in the absence of forcing (min)						
$T_d=\frac{\ln 2}{\mu}\approx 120$						

kinetic rate constants, and μ is the specific growth rate of the cells. Equation (1) describes the nonlinear interactions among the molecules controlling the cell cycle engine, while Eq. (2) describes cell growth. Equation (2) must be supplemented by a cell divison rule, $m\rightarrow\tau m$, where $0<\tau<1$, which divides the cell whenever the activity of the cyclin-dependent kinase (CDK) drops below a threshold $x_{cdk,thr}$ [33].

Based primarily on genetic studies of the cell cycle, detailed mathematical models for different organisms have been developed. Because of the homology of the key regulatory proteins, the core of the cell cycle regulation networks in different organisms operate quite similarly. Therefore, a minimal mathematical model of the cell cycle is expected to display the generic features of the detailed models describing cell cycles in different organisms [34].

Let us consider the following minimal model of the cell cycle,

$$\frac{dX}{dt}=m(k_1+k_2W)-(k_3+k_4Y+k_5Z)X, \tag{3}$$

$$\epsilon_Y\frac{dY}{dt}=\frac{(k_6+k_7Z)(1-Y)}{J_1+1-Y}-\frac{(k_8m+k_9X)Y}{J_1+Y}, \tag{4}$$

$$\frac{dZ}{dt}=(k_{10}+k_{11}X)-k_{12}Z, \tag{5}$$

$$\epsilon_W\frac{dW}{dt}=\frac{X(1-W)}{J_2+1-W}-\frac{PW}{J_2+W}. \tag{6}$$

In the terminology of the budding yeast cell cycle [35–37], X stands for the cyclin-dependent kinase activity, Y stands for the activity of Cdh1, Z stands for the activity of Cdc20, and W stands for the activity of the transcription factor, Mcm1, that controls the expression of the cyclin partner of CDK. Equation (3) and Eq. (5) are given by simple mass action laws, while Eqs. (4) and (6) describe the Michaelis-Menten enzymatic reactions for the regulations of Y and W.

III. PERIODIC FORCING OF THE CDK ENGINE

In the absence of forcing, cell cycle progression can be understood by considering the dynamics of Eq. (1) at fixed mass values, and then considering how $m(t)$ changes as cells grow and divide [38]. Equation (1) typically shows bistable dynamics at small m and oscillatory dynamics at intermediate m [33] for different specific models and parameter sets. Thus, our concern here is how forcing affects bifurcation points for bistable and oscillatory dynamics. For mathematical convenience, let us simplify Eqs. (3)–(6) into a two variable model,

$$\frac{dX}{dt}=m(k_1+k_2W^*)-(k_3+k_4Y^*+k_5Z)X, \tag{7}$$

$$\frac{dZ}{dt}=(k_{10}+k_{11}X)-k_{12}Z, \tag{8}$$

where,

$$W^*=G(X,\,P,\,J_2,\,J_2), \tag{9}$$

$$Y^*=G(k_6+k_7Z,\quad k_8m+k_9X,\,J_1,\,J_1). \tag{10}$$

Equations (7) and (8) are obtained from Eqs. (3)–(6) in the limit of $\epsilon_Y\rightarrow 0$ and $\epsilon_W\rightarrow 0$, by quasistationary assumptions $W(t)=W^*(X)$ and $Y(t)=Y^*(X,\,Z)$. W^* and Y^* are given by the Goldbeter-Koshland function [3],

$$G(a,b,c,d)=\frac{2ad}{b-a+bc+ad+\sqrt{(b-a+bc+ad)^2-4ad(b-a)}}. \tag{11}$$

The stationary solutions of Eqs. (7) and (8) can be found via nullcline intersections. Depending on the parameters, there can be either one, two or three steady states. If the parameter m is small, the system displays bistability, while if the mass is sufficiently large, there is a single steady state that can be unstable to oscillations. Such a dependence of number of steady states on mass is a generic feature of the cell cycle models [18]. Using the corresponding parameter values presented in Table I, we show in Fig. 1 the nullclines of Eqs. (7) and (8), as well as birhythmicity—two stable oscillations with different periods and amplitudes. We refer the readers interested in more about birhythmicity to Refs. [3,19,20].

Bifurcation diagrams are powerful tools for understanding cell cycle dynamics. Interestingly, the cell cycle models described by Eq. (1) display similar bifurcation diagrams in wide regions of kinetic rates, which typically involve a

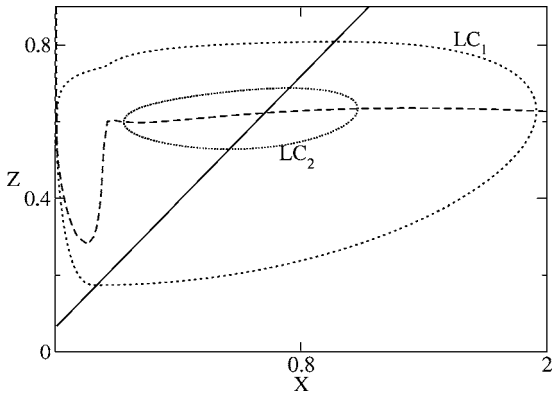

FIG. 1. Nullclines and birhythmicity in Eqs. (7) and (8). Dashed line; X nullcline, solid line; Z nullcline. Two dotted circles, marked by LC_1 and LC_2, show two stable limit cycle oscillations. Mass is fixed at $m=4.2$.

saddle node (SN), a saddle node invariant circle (SNIC), Hopf bifurcations (HB), and cyclicfold (CF) bifurcations. For example, although Eqs. (7) and (8) are unrealistic and too simplified for modeling the real physiology of the cell cycle, the two variable system displays similar bifurcations as Eqs. (3)–(6).

In Fig. 2 we show a bifurcation diagram for Eqs. (7) and (8) with the cell mass as the principal bifurcation parameter. At small mass and the low activity of cyclin-dependent kinase, there is a stable steady state which gives way to large amplitude oscillations at a SNIC bifurcation [20]. The dotted curve with the arrows in Fig. 2 shows the evolution of X and m in the course of progression through the cell cycle. This curve is computed from Eqs. (7) and (8) with the mass growth equation [Eq. (2)] and the mass division rule ($\tau=0.5$). When the curve with arrows is close to the solid line of the stable steady states with small values of X, the control system is in the G_1 phase of the cell cycle. As m grows, the control system passes the SNIC bifurcation at m_{SNIC} and the cell enters the S phase. As mass increases further, the curve

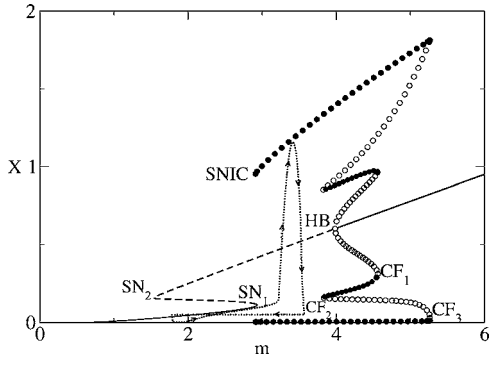

FIG. 2. A bifurcation diagram of Eqs. (7) and (8). Solid line; stable steady state, dashed line; unstable steady state, open circles; unstable oscillations, filled circles; stable limit cycles. The dotted curve with arrows shows the trajectory of motion when Eqs. (7) and (8) are supplemented by the mass growth equation, $\dot{m}=\mu m$. The cell divides ($m\rightarrow \tau m$) when X drops below $X_{thr}=0.05$; hence the trajectory undergoes an abrupt horizontal jump to the left at $X=X_{thr}$.

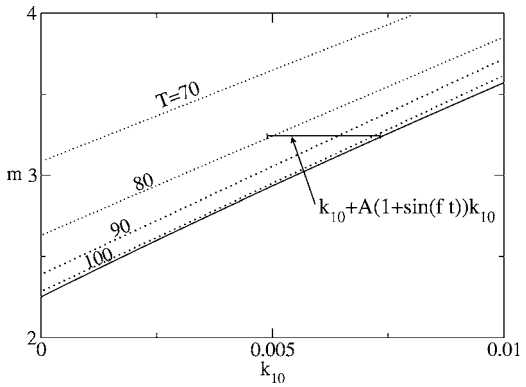

FIG. 3. Two parameter bifurcation diagram. The solid line is the continuation of the SNIC bifurcation. Dotted lines separate regions with different oscillation periods (T). Also indicated is a range of perturbation of k_{10}.

with arrows is captured by the stable limit cycle. As a result, X increases abruptly, driving the cell into a mitotic phase, then X drops below $X_{thr}=0.05$, causing the cell to divide and the control system returns to the stable G_1 phase.

In Fig. 3 we show the continuation of the SNIC bifurcation point in the parameter plane (m,k_{10}), where k_{10} is the synthesis rate of Cdc20. Let us consider a periodic modulation $k_{10}\rightarrow k_{10}+\delta k_{10}$, where $\delta k_{10}=Ak_{10}[1+\sin(ft)]$. Figure 3 suggests that the forced system can move from an initially oscillatory state to a stable steady state. Thus, the periodic modulation of k_{10} can affect the cell cycle progression, as the bifurcation point m_{SNIC} marks the checkpoint for the G_1–S transition. Indeed, simulations at $m\approx m_{SNIC}$ show that forcing leads to emergent, small amplitude, slow oscillations near the steady state, as shown in Fig. 4. Such emergent oscillations affect the cell cycle progression by increasing the interdivision time.

Obviously, k_{10} is not the only parameter whose modulations can shift bifurcation points. For example, the location of the cyclicfold bifurcation, CF_2, depends on the parameter k_2 [36,37]. Interestingly, at some interval of mass m, the system is monorhythmic, but it displays either large amplitude or small amplitude oscillations depending on the value

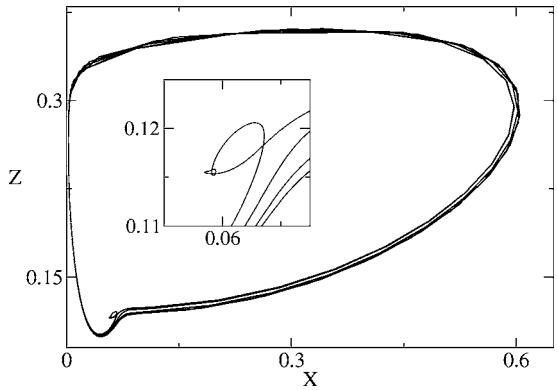

FIG. 4. Emergent orbits. Forcing may induce small amplitude, slow oscillations near the steady state. The inset magnifies the region of the small amplitude oscillations near the steady state. The parameters are: $m=3.2$, $A=0.4$, and $f=0.003$.

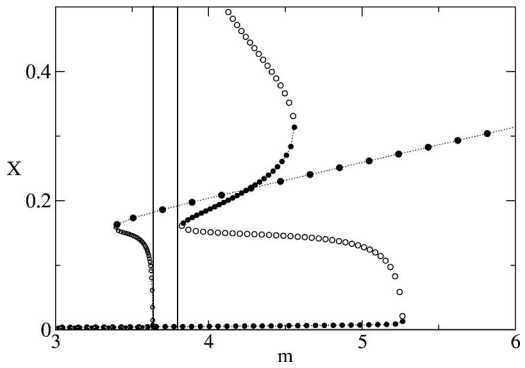

FIG. 5. Cyclicfold bifurcations at $k_2=0.0689$ (left) and $k_2=0.0795$ (right). Open circles indicate unstable oscillations, filled circles indicate stable oscillations. In the interval between the two vertical solid lines, the system is monorhythmic but oscillates on either a small or a large amplitude orbit depending on k_2.

of k_2, as in Fig. 5. Therefore, periodic modulations of $k_2 \rightarrow k_2+\delta k_2$, $\delta k_2=Bk_2[1+\sin(ft)]$ can switch the system between orbits of fast and slow oscillations.

Periodic forcing of the rate constant k_{10} can be achieved experimentally by putting a copy of the Cdc20 gene under the control of a *GAL* promoter. By periodically shifting the culture between galactose and glucose media, the *GAL* promoter can be turned on and off, respectively. These nutrient shifts will also cause the growth rate of the cells to change periodically from smaller to larger values in galactose and glucose media, respectively.

IV. FORCING A MINIMAL MODEL OF CELL CYCLE

In this section we study the periodic forcing of a minimal model of the cell cycle which includes mass growth and cell division. Experimentally, a simple way of forcing the cell cycle is by the periodic modulations of the growth medium. Because protein levels controlling the cell cycle depend on the cell's mass, modulations of the growth medium can indirectly affect the dynamics of the cell cycle engine. On the other hand, a localized perturbation of the cell cycle engine can be carried out by periodic modulations of the levels of the inducers and suppressors of the genes of the proteins involved in cell cycle regulation. Note that perturbations using the *GAL* promoter will necessarily entail a concomitant perturbation of growth rate.

For simplicity, consider the modulations of the synthesis rate of only a single protein in a minimal cell cycle model,

$$\frac{dX}{dt} = m[k_1 + k_2 G(X,P,J_2,J_2)] - (k_3 + k_4 Y + k_5 Z)X, \tag{12}$$

$$\frac{dY}{dt} = \frac{(k_6 + k_7 Z)(1-Y)}{J_2 + 1 - Y} - \frac{(k_8 m + k_9 X)Y}{J_2 + Y}, \tag{13}$$

$$\frac{dZ}{dt} = k_{10} + \delta k_{10} + k_{11} X - k_{12} Z. \tag{14}$$

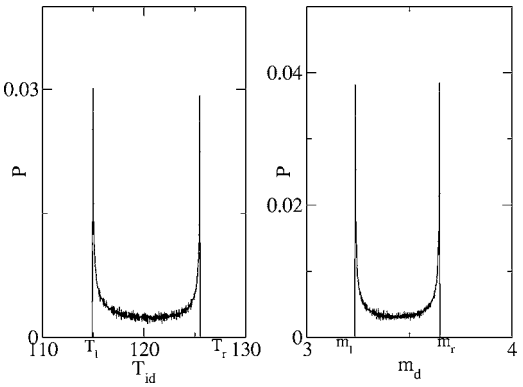

FIG. 6. A typical case of probability distributions of mass doubling time and mass at division at weak forcing.

$$\frac{dm}{dt} = (\mu + \delta\mu)m, \tag{15}$$

where, $\delta k_{10}=Ak_{10}[1+\sin(ft)]$ and $\delta\mu=B\mu[1+\sin(ft+\psi_0)]$, with $A \geqslant 0$ and $B \geqslant 0$. In the absence of forcing, Eqs. (12)–(15) describe an important module in a detailed model of a budding yeast [35]. We note that Eqs. (12)–(15) have been used in our previous publications, with $\delta k_{10}=0$ and $\delta\mu=0$, to model the effects of extrinsic noise and diffusion [36,37].

In the absence of forcing, the mass divides periodically as X regularly drops below X_{thr}. Thus when $A=B=0$, the interdivision time and mass at division are constants. At sufficiently strong forcing, however, these two quantities fluctuate and the probability distributions of these two quantities change from delta functions to bimodal distributions, as in Fig. 6. The sharp maxima at the edges of the distributions are due to the fixed value of X_{thr}. If the threshold is a random number with the mean X_{thr} and a certain variance, the maxima are not sharp as in Fig. 6.

Let us define the widths of the probability distributions by $\Delta T=T_r-T_l$ and $\Delta m=m_r-m_l$, where T_l, m_l, T_r, and m_r are defined in Fig. 6. For simplicity let $B=0$. We found that if the forcing frequency and amplitude are small, ΔT and Δm increase linearly with the increase of the intensity of forcing A. Such a linear dependence is due to the relationship between k_{10} and m along the SNIC curve which marks the G_1—S checkpoint, as in Fig. 3. Obviously, a SNIC bifurcation point can be continued on any two-dimensional parameter plane, using mass and a reaction rate other than k_{10}, as the bifurcation parameters. Therefore, the linear relationships, ΔT and Δm versus A, are expected when other reaction rates are perturbed.

In Fig. 7 we project on the (Y,X) plane snapshots of different irregular oscillations in Eqs. (12)–(15). Figure 7(a) shows a period-doubling bifurcation which occurs when the frequency and amplitude of forcing are small. It implies that, as a result of forcing, cells divide at larger or smaller mass than at $A=0$. Figure 7(b) shows toruslike motions which occur at small A and $f>0.6$. Such emergent toruslike motions originate from small amplitude, slow oscillations close to the steady state, as seen in Fig. 4. A period-three orbit that also

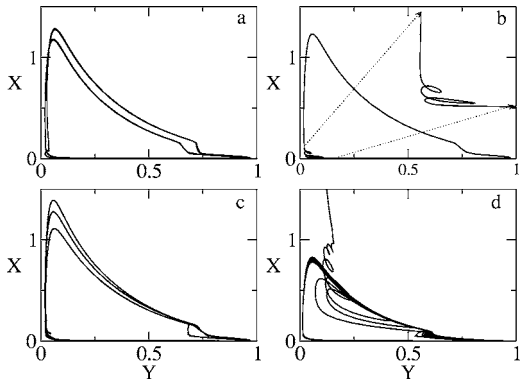

FIG. 7. Emergent orbits in Eqs. (12)–(15). (a) Period doubling. (b) Toruslike motion. (c) A combination of bifurcations shown in (a) and (b). (d) Cell cycle arrest.

involves toruslike motions at small X is shown in Fig. 7(c). Chaotic switching between birhythmic orbits are possible if parameters are chosen such that the distance between the orbits is sufficiently small. However, if the distance between the orbits is large, a cell cycle arrest may occur, Fig. 7(d). This happens because X cannot drop below the threshold when oscillations stay near the orbit of fast oscillations. As a result, m grows without division, leading to cell cycle arrest. The dynamics shown in Fig. 7 depend on the initial phase of forcing, on intial values X_0, Y_0, and Z_0, and on X_{thr}. For example, if X_{thr} is small, the cell cycle arrests are likely, whereas if it is sufficiently large, switching between the birhythmic orbits are more likely.

Depending on the emergent orbits, the interdivision time and the mass at division vary. Figure 8 shows periodically driven oscillations in Eqs. (12)–(15). The solid curve shows the cell division at discrete mass values, as the system displays a period-three orbit that includes toruslike motions [see Fig. 7(c)]. We know that with an increase of A, the probability distributions of mass at the division and interdivision time change from delta functions to distributions like those in Fig. 6. With a further increase of A, at the onset of the emergent orbits (Fig. 7), there is a transition when the probability distributions split into isolated distributions, Fig. 9.

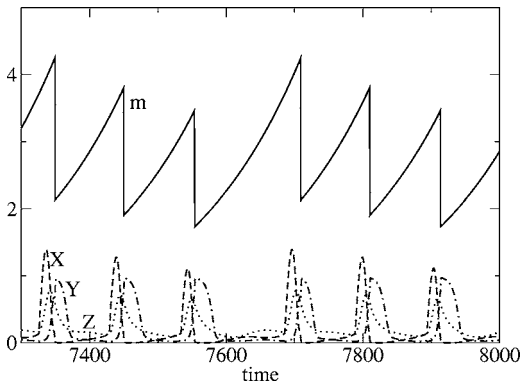

FIG. 8. Cell division under periodic forcing. Solid line shows periodically modulated mass dynamics. Other lines show the oscillations of X, Y, and Z, respectively. Parameters are as in Table I, except $A=1$, $f=0.07$ (4:3 resonance), $X_{trh}=0.05$, $k_{10}=0.0025$, and $B=0$.

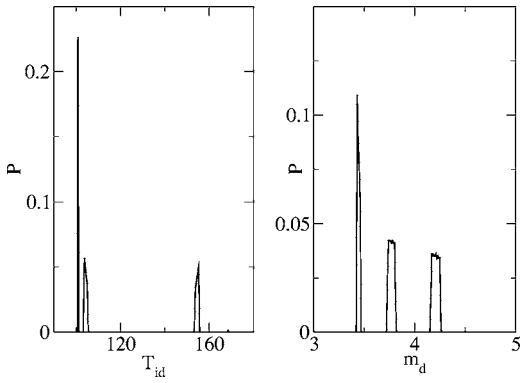

FIG. 9. Splitting of the probability distributions. Parameters are the same as in Fig. 8.

Our simulations show that if $A\neq 0$ and $B\neq 0$, the interval for the parameters A and B leading to splitting of the probability distributions is narrow. Also the isolated probability distributions are stable only if $B\ll A$. The reason is that the parameter B modulates the interdivision time T_d, narrowing the resonance conditions. In fact, when $A\neq 0$ and $B=0$, a splitting of the probability distributions occurs when the period of forcing is a rational multiple of T_d.

Note that the results presented in this section do not depend on the wave form of the forcing function or the relative phase ψ_0. For instance, the linear relationships between the widths of the probability distributions and A, as well as the splitting of the probability distributions, have been observed when we replace the sine wave by rectangular wave trains.

V. MODE LOCKING

Based on one's previous knowledge of forced oscillatory systems [2], one would guess that the splitting of probability distributions is associated with resonance, when the unperturbed oscillation frequency is a rational multiple of the forcing frequency. Such a motion is also called mode locking and it has a negative Lyapunov exponent indicating its periodic nature. Thus, in order to show that the splitting of probability distributions is associated with mode locking, we need to calculate the Lyapunov exponents of Eqs. (12)–(15). However, for systems like Eqs. (12)–(15), which have temporal discontinuties when the cell divides, the calculation of the Lyapunov exponents is quite complicated. Using a method developed in Ref. [39], we numerically compute the maximal Lyapunov exponent of Eqs. (12)–(15). We find that $\lambda=-0.000\,12$ for the dynamics shown in Fig. 9, whereas, for the unperturbed orbit (Fig. 2, $A=B=0$), λ is vanishing.

In Fig. 10 we show a series of cases when $A=B\approx 1$. For each value of A, we record a time interval during which the cell divides 1000 times. The first row shows the distribution of the interdivision times, T^n, and the second row shows the distribution of mass at division, m_d. At values of A, where the spectra are continuous, the probability distributions are similar to the distributions shown in Fig. 6. At values, where spectra are discrete, the probability distributions are similar to Fig. 9. The third row shows the corresponding maximal Lyapunov exponents. As expected, the minimum of λ is lo-

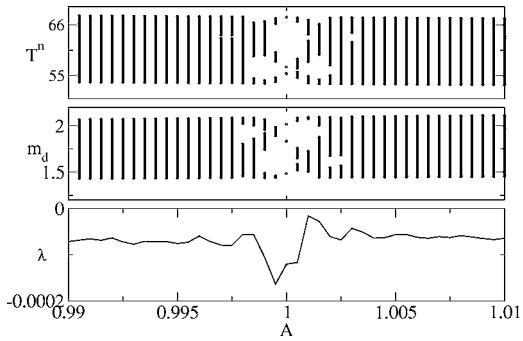

FIG. 10. A bifurcation diagram of T^n and m_d, and the corresponding Lyapunov exponents for Eqs. (12)–(15). The parameters are the same as in Fig. 9 except $A=B$, $f=0.035$ (2:3 resonance), and $k_2=0.0795$.

cated in the area where the system is in a mode-locked regime.

According to Fig. 10, when $A=B\approx 1$, the parameter window for mode-locked solutions in Eqs. (12)–(15) is quite narrow ($\pm 0.2\%$) as discussed in the previous section. We found that mode locking occurs in a wider parameter interval ($\pm 5\%$) for the periodic forcing of an "integrate-and-fire" model [2] of the cell cycle. In this toy model, mass growth is given by

$$\frac{dm}{dt} = \mu m + B\mu[1+\sin(ft)]. \tag{16}$$

The cell divides at time $T^{(n)}$ when m reaches the threshold $h(t)$,

$$m_-(T^{(n)}) = \lim_{\epsilon\to 0} m(T^{(n)}-\epsilon) = h(t) = m^* + A[1+\sin(ft+\psi_0)]. \tag{17}$$

At time $T^{(n)}$, mass is reduced by a factor $\tau \in (0,1)$

$$m_+(T^{(n)}) = \lim_{\epsilon\to 0} m(T^{(n)}+\epsilon) = \tau h(t). \tag{18}$$

In Eq. (17) by forcing the threshold we imply forcing of the cell cycle engine. m^* is constant and $T^{(n)}$ is defined as,

$$T^{(n)} = inf\{t | m(t) \geqslant h(t); t \geqslant T^{(n-1)}\}. \tag{19}$$

Note the difference between the forcing terms in Eq. (15) and Eq. (16). Following [28,40] , we calculate the Lyapunov exponent of Eqs. (16)–(19),

$$\lambda = \mu + \lim_{n\to\infty} \frac{1}{T^{(n)}-T^{(0)}} \sum_{j=1}^{n} \ln \tau \left| \frac{\mu m + \tau^{-1} B[1+\sin(fT^{(j)})] - fA\cos(fT^{(j)}+\psi_0)}{\mu m + B[1+\sin(fT^{(j)})] - fA\cos(fT^{(j)}+\psi_0)} \right|. \tag{20}$$

The system is periodic, quasiperiodic, and chaotic if $\lambda<0$, $\lambda=0$, and $\lambda>0$. In Eq. (20), the first component accounts for the continuous growth between cell divisions, while the second component accounts for mass resets at the cell divisions.

In the absence of forcing, i.e., when $A=B=0$, the time after the n division is $T^{(n)}=nT_d$. Assuming $T^{(0)}=0$, we find from Eq. (20) that $\lambda=\mu+(\ln\tau)/(T_d)=0$. If $B=0$ and $A\neq 0$, λ can be negative only if $T^{(n)}<T_d$. Also from Eq. (20) we see that λ can be negative if $B\neq 0$.

The first two rows of Fig. 11 show distributions of the time interval between divisions, T^n, and mass at division, m_d, upon variations of A in Eqs. (16)–(19). Continuous spectra at a fixed A give probability distributions similar to Fig. 6, whereas discrete spectra give probability distributions similar to Fig. 9. The last row of Fig. 11 reports the corresponding Lyapunov exponents computed from Eq. (20), which show that the discrete spectra are associated with the negative values of λ. Note that, in contrast to Fig. 10, the mode locking interval is wider in Fig. 11. Our simulations confirm that the mode locked solution is in 5:2 resonance. The cell number in a culture cannot increase indefinitely. Therefore, n is a finite number in our computations of Eq. (20). We think that the slightly positive values of λ in Fig. 11 are due to the numerical approximations associated with the finiteness of n. Thus, at these values of λ the oscillations are quasiperiodic.

VI. DISCUSSION

Cell cycle division is driven by a cell cycle "engine," a reaction network that involves many genes and proteins. The engine is not a totally autonomous system, it interacts with other reaction networks and with the environment. A very interesting problem is whether cell cycle rhythms can be controlled by other oscillatory processes in the cell, or by periodic perturbations of environmental parameters.

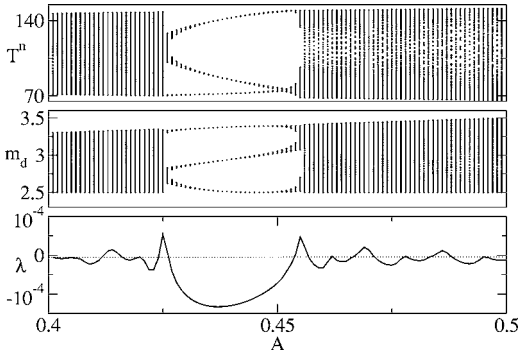

FIG. 11. The bifurcation diagrams of T^n and m_d, and the corresponding Lyapunov exponents of Eqs. (16)–(19). Parameters are $f\approx 0.0209$, $m^*=2.5$, $\psi_0=0$, and $A=B$.

In this work we considered the case, where the protein involved in cell cycle regulation, is periodically modulated by an inducer of its gene, and where such perturbations are associated with the modulations of cell growth rate. Under these conditions, we studied the effects of periodic forcing in a minimal mathematical model of the yeast cell cycle. In proliferating diploid yeast strains, interactions between the cells are weak [35] and single cells behave independently. In this case, probability distributions of interdivision time and mass at a division calculated for a single cell over time can be equated to the distributions characterizing a whole population of cells at a given time. Our results show that if the amplitude and frequency of the forcing is small, the width of the distributions increases linearly with an increase of the forcing amplitude. However, at stronger forcing amplitudes and at some forcing frequencies, the probability distributions may split into isolated distributions. By computing Lyapunov exponents we showed that the splitting of the probability distributions is associated with mode-locked solutions.

Although we considered a minimal model, our results are expected to carry over into more detailed cell cycle models. Indeed, in a recently published paper, Cross and Siggia studied mode locking in a more elaborate model of the budding yeast cell cycle [41]. Our work uncovers some features of mode locking in the cell cycle that are missing from the paper by Cross and Siggia. First, we point out that the periodic expression of a gene product from a *GAL* promoter affects not only the rate of expression of the protein but also the growth rate of the medium, because cells grow faster in glucose than they do in galactose. If we assume that $\dot{m} = \mu m$ and periodically perturb μ, then the mode locking windows are narrow. If we assume $\dot{m} = \mu_0 + \mu m$ and periodically perturb μ_0 (as in the integrate and fire model), then the mode locking parameter windows are much wider. In addition, we demonstrate the stability of the mode-locked solution by computing the Lyapunov exponents.

The synchronization of periodic processes is a fundamental problem in science. Currently, synchronization and collective dynamics of biological cells and distributed oscillators are an active research area [42–47]. Our integrate-and-fire model for cell cycle progression can be useful in cell cycle synchronization studies as the model is analytically tractable. In the mode locking regime, cells can be synchronized. Our preliminary results show that a cell culture with cells, initially in random cell cycle phases, whose dynamics are described by Eqs. (3)–(6) can be synchronized by periodic forcing [48].

ACKNOWLEDGMENTS

The authors thank Kathy Chen for many fruitful discussions. This work was supported by grants from DARPA's Biocomputation Program (AFRL No. F300602-02-0572) and the James S. McDonnell Foundation (Grant No. 21002050).

[1] A. T. Winfree, *The Geometry of Biological Time*, 2nd ed. (Springer, New York, 2001).
[2] L. Glass and M. C. Mackey, *From Clocks to Chaos* (Princeton, New Jersey, 1988).
[3] A. Goldbeter, *Biochemical Oscillations and Cellular Rhythms* (Cambridge University Press, Cambridge, 1996).
[4] L. Glass, Nature (London) **410**, 277 (2000).
[5] T. Matsuo, S. Yamaguchi, S. Mitsui, A. Emi, F. Shimoda, and H. Okamura, Science **302**, 255 (2003).
[6] K. Nasmyth, Trends Genet. **12**, 405 (1996).
[7] J. J. Loros and J. C. Dunlap, Annu. Rev. Physiol. **63**, 757 (2001).
[8] K. C. Chen, L. Calzone, A. Csikasz-Nagy, F. R. Cross, B. Novak, and J. J. Tyson, Mol. Biol. Cell **15**, 3841 (2004).
[9] B. Novak and J. J. Tyson, J. Theor. Biol. **230**, 563 (2004).
[10] J. Leloup and A. Goldbeter, Proc. Natl. Acad. Sci. U.S.A. **100**, 7051 (2003).
[11] D. B. Forger and C. S. Peskin, Proc. Natl. Acad. Sci. U.S.A. **100**, 14806 (2003).
[12] F. R. Cross, V. Archambault, M. Miller, and M. Klovstad, Mol. Biol. Cell **13**, 52 (2002).
[13] W. Sha, J. Moore, K. Chen, A. D. Lassaletta, C. Yi, J. J. Tyson, and J. C. Sible, Proc. Natl. Acad. Sci. U.S.A. **100**, 975 (2003).
[14] M. P. S. Dekens, C. Santoriello, D. Vallone, G. Grassi, D. Whitmore, and N. S. Foulkes, Curr. Biol. **14**, R24 (2004).
[15] B. Raboy, A. Marom, Y. Dor, and R. G. Kulka, Mol. Microbiol. **32**, 729 (1999).
[16] M. P. S. Dekens, C. Santoriello, D. Vallone, G. Grassi, D. Whitmore, and N. S. Foulkes, Curr. Biol. **13**, 2051 (2003).
[17] M. R. Alexander, M. Tyers, M. Perret, B. M. Craig, K. S. Fang, and M. C. Gustin, Mol. Biol. Cell **12**, 53 (2001).
[18] A. Csikasz-Nagy, D. Battogtokh, B. Novak, and J. J. Tyson (unpublished).
[19] M. Stich, M. Ipsen, and A. S. Mikhailov, Physica D **171**, 19 (2002).
[20] M. T. Borisuk and J. J. Tyson, J. Theor. Biol. **195**, 69 (2000).
[21] D. Gonze and A. Goldbeter, J. Stat. Phys. **101**, 649 (2000).
[22] K. Aihara, G. Matsumoto, and Y. Ikegaya, J. Theor. Biol. **109**, 249 (1984).
[23] Y. Shinohara, T. Kanamaru, H. Suzuki, T. Horita, and K. Aihara, Phys. Rev. E **65**, 051906 (2002).
[24] A. Goldbeter, D. Gonze, G. Houart, J. Leloup, J. Halloy, and G. Dupont, Chaos **11**, 247 (2001).
[25] M. J. Chacron, A. Longtin, and K. Pakdaman, Physica D **192**, 138 (2004).
[26] M. Tsuchiya and J. Ross, Proc. Natl. Acad. Sci. U.S.A. **100**, 9691 (2003).
[27] C. R. Laing and A. Longtin, Phys. Rev. E **67**, 051928 (2003).
[28] S. Coombes and P. C. Bressloff, Phys. Rev. E **60**, 2086 (1999).
[29] E. E. Selkov, T. Chuluun, and D. Battogtokh, Stud. Biophys. **31**, 137 (1991).
[30] M. Marhl and S. Schuster, J. Theor. Biol. **234**, 491 (2003).
[31] B. Novak and J. J. Tyson, J. Theor. Biol. **165**, 101 (1993).
[32] B. Novak, Z. Pataki, A. Cilberto, and J. J. Tyson, Chaos **11**, 277 (2001).
[33] J. J. Tyson and B. Novak, J. Theor. Biol. **210**, 249 (2001).

[34] T. Alarcon, H. M. Byrne, and P. K. Maini, J. Theor. Biol. **229**, 395 (2004).
[35] K. Chen, A. Csikasz-Nagy, B. Georffy, J. Val, B. Novak, and J. J. Tyson, Mol. Biol. Cell **11**, 369 (2000).
[36] D. Battogtokh and J. J. Tyson, Chaos **14**, 653 (2004).
[37] D. Battogtokh and J. J. Tyson, Phys. Rev. E **70**, 026212 (2004).
[38] J. J. Tyson, A. Csikasz-Nagy, and B. Novak, BioEssays **24**, 1095 (2002).
[39] P. C. Muller, Chaos, Solitons Fractals **5**, 1671 (1995).
[40] S. Coombes, Phys. Lett. A **255**, 49 (1999).
[41] F. R. Cross and E. D. Siggia, Phys. Rev. E **72**, 021910 (2005).
[42] T. Zhou, L. Chen, R. Wang, and K. Aihara, Genome Informatics **15** (2), 233 (2004).
[43] L. Chen, R. Wang, T. Kobayashi, and K. Aihara, Phys. Rev. E **70**, 011909 (2004).
[44] Y. Kuramoto, D. Battogtokh, and H. Nakao, Phys. Rev. Lett. **81**, 3543 (1998).
[45] V. Casagrande and A. S. Mikhailov, Physica D **205**, 154 (2005).
[46] A. S. Mikhailov and V. Calenbuhr, *From Cells to Societies, Models of Coherent Action* (Springer, New York 2001).
[47] K. Kaneko and T. Yomo, J. Theor. Biol. **199**, 243 (1999).
[48] D. Battogtokh (unpublished).